Probing the sensitivity of nanowire-based biosensors using liquid-gating



2010 Nanotechnology 21 425505

(http://iopscience.iop.org/0957-4484/21/42/425505)

Nanotechnology **21** (2010) 425505 (5pp) doi:10.1088/0957-4484/21/42/425505

# Probing the sensitivity of nanowire-based biosensors using liquid-gating

**Ming-Pei Lu**[1,4], **Cheng-Yun Hsiao**[2,4], **Wen-Tsan Lai**[2] and **Yuh-Shyong Yang**[1,2,3]

[1] National Nano Device Laboratories, Hsinchu 300, Taiwan
[2] Institute of Biological Science and Technology, National Chiao Tung University, Hsinchu 300, Taiwan
[3] Instrument Technology Research Center, Hsinchu 300, Taiwan

E-mail: mingpei.lu@gmail.com and ysyang@faculty.nctu.edu.tw

Received 28 May 2010, in final form 2 September 2010
Published 24 September 2010
Online at stacks.iop.org/Nano/21/425505

**Abstract**

We have used liquid-gating to investigate the sensitivity of nanowire (NW)-based biosensors for application in the field of ultrasensitive biodetection. We developed an equivalent capacitance model of the biosensor system to explore the dependence of the sensitivity on the liquid-gate voltage ($V_{lg}$), which was influenced by capacitive competition between the NW capacitance and the thin oxide capacitance. NW biosensors with highest sensitivity were obtained when we operated the device in the subthreshold regime while applying an appropriate value of $V_{lg}$; the influence of leakage paths through the ionic solutions led, however, to significant sensitivity degradation and narrowed the operating window in the subthreshold regime.

(Some figures in this article are in colour only in the electronic version)

## 1. Introduction

Since the first one-dimensional (1D) nanomaterial-based biosensor was developed for biological and chemical sensing in 2001 [1], such systems have attracted increasing attention for their promising use as highly sensitive biosensors because of their high surface-to-volume ratios and sizes comparable with those of biomolecules [1–12]. Reports of such biosensors being used for the selective detection of viruses [2], antigens [3, 5], DNA [8], and other biological species [1, 6, 7, 9, 10] have appeared steadily over the past decade. At present, one of the most pressing issues is improving the sensitivity of these biosensors so that they may be used for the ultrahigh-sensitivity detection of only a single or a few biomolecules. During the preparation of this paper, Gao *et al* observed the improved sensitivity of a nanowire (NW)-based biosensor in the subthreshold regime [13]; nevertheless, there remains a lack of information regarding the physical correlation between the sensitivity of biosensor systems and their operating conditions. Herein, we reveal that the sensitivity of one such device can be modulated electrically, through liquid-gating, to its limit by applying an appropriate liquid-gate voltage ($V_{lg}$), thereby modifying the capacitive coupling effect in the biosensor system. We also describe the origin of the sensitivity degradation in the subthreshold regime.

## 2. Experimental details

In this study, n-type polycrystalline silicon (poly-Si) NWs, employed as 1D conducting channels to study the sensitivity of NW biosensors, were fabricated using fully complementary metal–oxide–semiconductor (CMOS)-compatible processes [10]. First, the starting Si substrate was covered with a 100 nm silicon oxide ($SiO_2$) layer and an 80 nm silicon nitride ($Si_3N_4$) layer. Next, a $SiO_2$-dummy gate structure (length, 2 $\mu$m; width, 500 nm) was formed on the substrate. Subsequently, an amorphous silicon (a-Si) layer (thickness, 100 nm) was deposited onto the substrate; the sample was then subjected to annealing at 600 °C to transform the a-Si into poly-Si. The poly-Si NWs and source/drain (S/D) contact areas were defined through a photolithography process and reactive plasma etching processing. Note that two sidewall poly-Si NW channels connected in parallel were formed along the edges of the dummy gate structure using the sidewall-spacer technique. The low-resistive poly-Si areas used for S/D

[4] These authors contributed equally to this work.

 

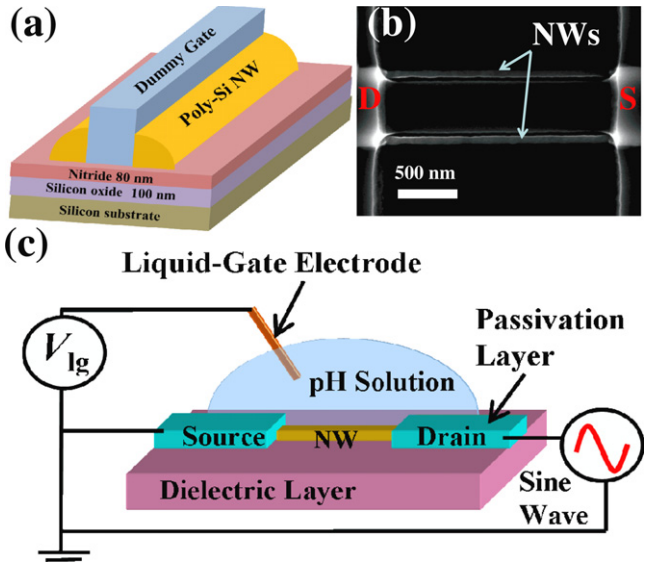


**Figure 1.** Representative diagrams of the NW device structure and the measurement setup. (a) Typical NW device structure, fabricated using the sidewall-spacer technique, revealing two NWs connected in parallel along the dummy gate edges. (b) Top-view SEM image of the NW device, revealing that it featured two NW channels connecting the S and D electrodes. (c) Conductance measurement setup of the liquid-gating NW device. The Au microwire that was inserted directly into the solution served as a liquid-gate electrode.

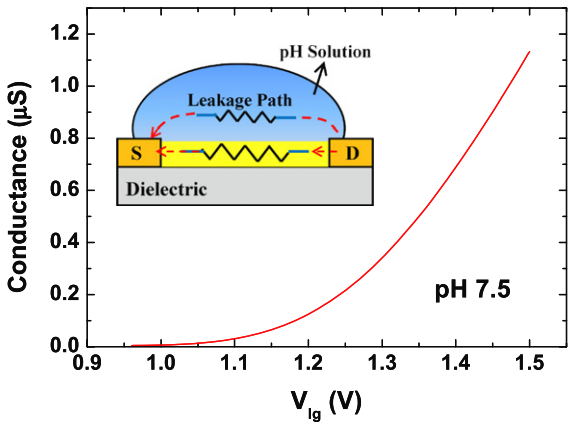


**Figure 2.** Experimental conductance of the NW device in the pH-7.5 solution, plotted with respect to $V_{lg}$. Inset: schematic representation of the equivalent circuit of the measured conductance, which was contributed mainly by the parallel connection of the inherent conductance of the two parallel NWs and the ionic conductance of the leakage paths through the solution.

contacts were fabricated through ion implantation. Finally, the S/D contacts were passivated by a 150 nm $SiO_2$ layer, thereby decreasing both the leakage current [14] and noise in the solution environment. A schematic representation of the NW device prepared using the sidewall-spacer technique is provided in figure 1(a). The top-view SEM image of the NW device in figure 1(b) reveals that the NW device featured two poly-Si NWs (lengths about 2 $\mu$m) connecting in parallel. The vertical thickness and height of the poly-Si NW were about 45 nm and about 70 nm, respectively, determined from a cross-sectional view transmission electron microscopy (TEM) image (not shown here).

Phosphate-buffered solutions (PBS, 10 mM) were prepared in deionized water; the pH was adjusted to a specific value using sodium phosphate monobasic and sodium phosphate dibasic (J T Baker, USA). In liquid-gating systems [15], a biosensor will have sufficiently high efficiency to modulate the inherent conductance of the NW through the gating effect if any surface potential changes occur at the solution–$SiO_2$ interface, induced by a change in the number of surface charged groups; therefore, we used such systems to investigate the sensitivity of our biosensors. The liquid-gate electrode comprised a gold (Au) microwire (this inert metal was used to suppress electrochemical reactions between the solution and the electrode) inserted into a solution of known pH. The conductance measurements were performed using the lock-in technique at room temperature. A sine wave (47 Hz; amplitude 10 mV) was applied to the drain electrode. The source electrode was connected virtually to the ground of the lock-in amplifier system. Figure 1(c) provides a schematic representation of the measurement setup for characterizing the conductance in the liquid-gating device. The measured conductance of the device increased upon increasing $V_{lg}$ from 0.96 to 1.5 V in the pH-7.5 solution (figure 2), indicating the typical electrical behavior of an n-type device in which electron carriers play the dominant role in current transport. The inset to figure 2 presents the equivalent circuit of the measured conductance in the liquid-gating NW device system; competition between the inherent conductance of the poly-Si NWs and the ionic conductance of the leakage paths would govern the measured conductance of the NW device. The threshold voltage ($V_{th}$) of this device, extracted through linear extrapolation, was 1.23 V.

## 3. Results and discussion

To change the surface potential at the solution–$SiO_2$ interface, and, thereby, to evaluate the sensitivity of the NW biosensor, we increased the degree of deprotonation of the silanol (SiOH) groups by varying the pH from a low to high value to increase the density of negatively charged groups ($SiO^-$) [1, 16], as illustrated in figure 3(a). We performed real-time conductance measurements to observe the change in conductance caused by the change in surface potential at the solution–$SiO_2$ interface upon increasing the pH from 7.5 to 8.5. Initially, we used a syringe pump to deliver the pH-7.5 solution into direct contact with the NW. When the conductance of the device became electrically stable, the pH-7.5 solution was replaced by the corresponding pH-8.5 solution. We positioned an air bubble (about 50 $\mu$l) intentionally between the two different solutions. As this bubble flowed across the surface of the NW, we observed in real-time that the electrical signal was disturbed, confirming that the change in solution pH occurred simultaneously with the change in the signal. We measured the conductance of the device under pH changes from 7.5 to 8.5 at various values of $V_{lg}$. Figure 3(b) presents the data normalized to $\Delta G/G_{pH-7.5}$ for comparison. The conductance of the n-type NW device decreased upon increasing the pH

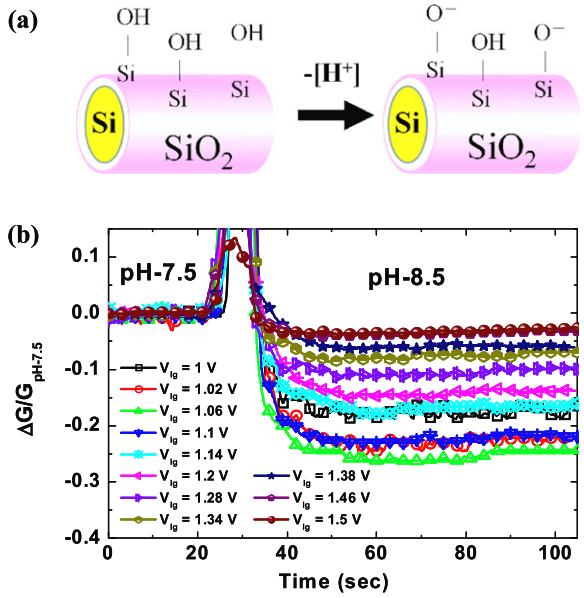


**Figure 3.** (a) Schematic representation of the deprotonation of SiOH groups on the NW surface upon increasing the pH. (b) Real-time $\Delta G/G_{\mathrm{pH-7.5}}$ curves for pH changes from 7.5 to 8.5 at various values of $V_{\mathrm{lg}}$. An air bubble, placed intentionally between the pH-7.5 and pH-8.5 solutions, caused the initial disturbance of the electrical signals.

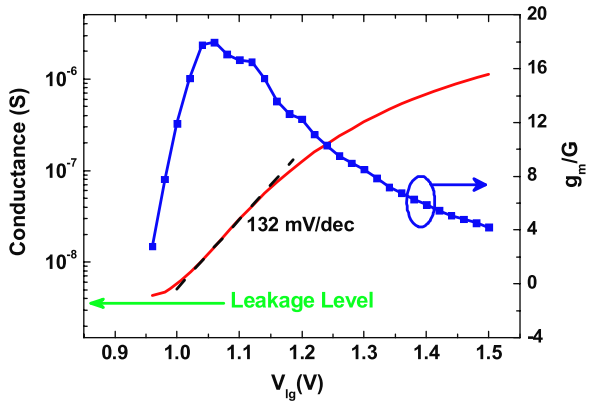


**Figure 4.** Left-hand axis: semilogarithmic plot of the $G$–$V_{\mathrm{lg}}$ curve for the device in the pH-7.5 solution (red line). The extracted value of the subthreshold swing is 132 mV/dec. The magnitude of the ionic conductance contributed by the leakage paths through the solutions in our case is labeled (green line). Right-hand axis: plot of $g_{\mathrm{m}}/G_{\mathrm{pH-7.5}}$ with respect to $V_{\mathrm{lg}}$, using data obtained from the $G$–$V_{\mathrm{lg}}$ curve.

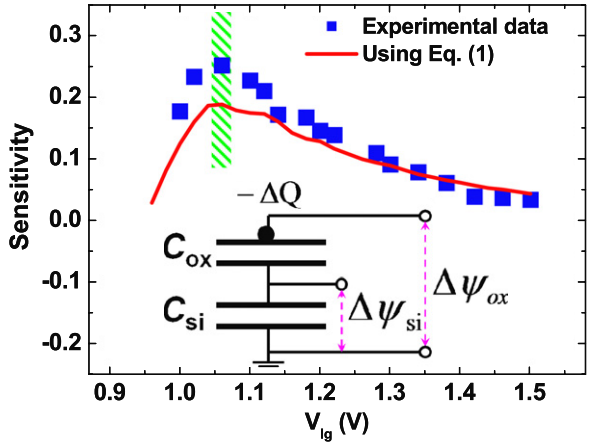


**Figure 5.** Comparison of the experimental data for the pH sensitivity (■) and the fitting curve (red solid line) obtained using equation (1). Inset: equivalent capacitive model of the solution/NW system. The increased negative charge ($-\Delta Q$) due to deprotonation at the oxide surface is labeled in the circuit.

from 7.5 to 8.5; we attribute this behavior to the presence of additional negative charges at the $SiO_2$ surface. According to previous reports [1, 5, 12, 17], the conductance of p-type NW devices will increase upon increasing the pH from low to high values—opposite to the trend we observed for our n-type system. Furthermore, the value of $\Delta G/G_{\mathrm{pH-7.5}}$ of our NW device could be controlled electrically by varying the value of $V_{\mathrm{lg}}$, as indicated in figure 3(b). Figure 4 presents a semilogarithmic plot of the conductance of the device with respect to the value of $V_{\mathrm{lg}}$ in the pH-7.5 solution. The subthreshold swing of this device was extracted to be as high as 132 mV/dec. Moreover, the measured conductance was weakly dependent on the value of $V_{\mathrm{lg}}$ when the device was operated in the low conductance regime, as indicated in figure 4, suggesting that the ionic conductance of the leakage paths played a major role in the measured conductance. The magnitude of the ionic conductance contributed by the leakage paths in our NW device reached as high as about $4 \times 10^{-9}$ S, as denoted in figure 4. Furthermore, figure 5 plots the experimental sensitivity of the NW device, defined as $\Delta G/G_{\mathrm{pH-7.5}}$ (calculated by averaging the real-time conductance responses depicted in figure 2), with respect to $V_{\mathrm{lg}}$. The highest sensitivity of the NW biosensor occurred in the subthreshold regime, with the sensitivity decreasing upon further increasing the value of $V_{\mathrm{lg}}$; figure 5 reveals a sevenfold enhancement in sensitivity for the NW device operated in the subthreshold regime relative to that in the above-threshold regime. Understanding the cause of the dependence of the sensitivity on the value of $V_{\mathrm{lg}}$ in the liquid-gating NW device will require further investigation.

To simplify the quantitative model of sensitivity, we focus herein on the relationship between the sensitivity and the surface potential at the solution–$SiO_2$ interface. Physically speaking, there are three capacitances connected in series within this solution/NW system: the electrical double-layer capacitance ($C_{\mathrm{DL}}$), the thin oxide layer capacitance ($C_{\mathrm{ox}}$), and the capacitance of the nanowire ($C_{\mathrm{NW}}$). The Debye screening length for 10 mM PBS is about 3 nm, comparable with the thickness of the thin oxide layer (thickness of 2–3 nm in our case). In addition, the dielectric constant of the electrical double-layer (about 80) was more than 20 times greater than that of $SiO_2$ (about 3.9) [14]. This situation suggested that $C_{\mathrm{DL}}$ would be substantially greater than $C_{\mathrm{ox}}$, indicating that $C_{\mathrm{ox}}$ would play a dominant role in determining the values of those two $V_{\mathrm{lg}}$-independent capacitances connected in series between the NW and the liquid-gate electrode. Finally, the equivalent capacitive model can be simplified as $C_{\mathrm{ox}}$ serially connected to $C_{\mathrm{NW}}$; thus, the value of $\Delta\psi_{\mathrm{ox}}$ (the surface potential change at the solution–$SiO_2$ interface) can essentially be considered as

the value of $\Delta V_{lg}$. Relative to the slope of $G$, which varied dramatically with respect to $V_{lg}$ in the subthreshold regime, the slope of $G$ in the above-threshold regime varied only slightly with respect to $V_{lg}$, as indicated in figure 4. Therefore, the sensitivity ($S$) for the NW biosensor operated in the above-threshold regime can be defined as

$$S = \left| \frac{\Delta G}{G_{\mathrm{pH-7.5}}} \right| \approx \left| \frac{g_m}{G_{\mathrm{pH-7.5}}} \Delta \psi_{\mathrm{ox}} \right| \quad (1)$$

where $g_m$ and $G_{\mathrm{pH-7.5}}$ are the transconductance and conductance, respectively, of the device in the pH-7.5 solution. Figure 4 reveals that the $g_m/G_{\mathrm{pH-7.5}}$ curve obtained from the $G$–$V_{lg}$ data is a function of $V_{lg}$. To extract the value of $\Delta\psi_{\mathrm{ox}}$, we fitted the experimental data for the sensitivity at various values of $V_{lg}$ in the above-threshold regime using equation (1), in which $\Delta\psi_{\mathrm{ox}}$ is the only fitting parameter. Figure 5 compares the experimental results with the fitting curve, providing an extracted value of $\Delta\psi_{\mathrm{ox}}$ of about $-10.5$ mV for the pH change from 7.5 to 8.5; this agrees well with the value reported in the literature for the pH sensitivity of the $SiO_2$ surface [18]. In addition, relative to the ideal value, based on the Nernst equation, of $-60$ mV/pH, the absolute value of our system is low, presumably because of the dependence of $\Delta\psi_{\mathrm{ox}}$ on the site density and dissociation constant of the SiOH groups [16].

The NW biosensor exhibited optimal sensitivity when we applied a value of $V_{lg}$ of 1.06 V, which corresponded approximately to the maximum value of $g_m/G_{\mathrm{pH-7.5}}$, as labeled by the green shadow in figure 5. Using the expression $G \sim \exp(\alpha e V_{lg}/k_B T)$ for an NW biosensor operating in the subthreshold regime [15], the correlation between $g_m/G_{\mathrm{pH-7.5}}$, $\Delta G$, and $G_{\mathrm{pH-7.5}}$ can be given as

$$\frac{\partial \Delta G}{\partial V_{lg}} \frac{1}{G_{\mathrm{pH-7.5}}} = \frac{g_m}{G_{\mathrm{pH-7.5}}} [1 - \exp(\alpha e \Delta\psi_{\mathrm{ox}}/k_B T)]. \quad (2)$$

Accordingly, $g_m/G_{\mathrm{pH-7.5}}$ is proportional to the differential conductance change divided by the conductance, indicating that it can essentially be correlated to the sensitivity of the NW biosensor. Therefore, it suggests that we have developed a new methodology for optimizing the sensitivity of NW biosensors: by applying an appropriate value of $V_{lg}$ that has been extracted from the $g_m/G$ curve. Note that the device-to-device variations in the threshold voltages and electrical performances of the electronic devices cannot be ignored when their feature sizes are decreased to the nano-scale, especially in the case of NW devices. Therefore, it remains highly unlikely that we could control all NW biosensors, fabricated using the same fabrication process flow, so that they operate with similar sensitivity performances when applying the same operational bias conditions. How we can optimize the sensitivity of NW biosensors prior to performing the biological measurements is, therefore, an important issue for the practical application of NW biosensors. Thus, we have demonstrated a method for evaluating the sensitivity of NW biosensors using solutions of various values of pH; this approach can be applied practically to the field of highly sensitive NW biosensors.

To further investigate the dependence of the sensitivity on the value of $V_{lg}$ in the NW device, as plotted in figure 5, we divided the whole sensitivity into two stages. In the first stage, the sensitivity of the NW device decreased as the value of $V_{lg}$ increased beyond 1.06 V. We attribute this behavior mainly to the potential coupling effect between all effective capacitances connected in series within the liquid-gating system. The inset to figure 5 displays the equivalent capacitive model, comprising $C_{ox}$ and $C_{NW}$, that we used to explore the correlation between the sensitivity of the NW biosensor and the capacitive coupling effect in the solution/NW system. The increased negative charge ($-\Delta Q$) due to deprotonation at the oxide surface is also labeled in the circuit. The coupling ratio ($\alpha$) of the surface potential change in the NW to the liquid-gate voltage change, based on the capacitive model, can be given as

$$\alpha = \frac{\Delta\psi_{\mathrm{NW}}}{\Delta V_{lg}} \approx \frac{\Delta\psi_{\mathrm{NW}}}{\Delta\psi_{\mathrm{ox}}} = \frac{C_{\mathrm{ox}}}{C_{\mathrm{ox}} + C_{\mathrm{NW}}} \quad (3)$$

where $\Delta\psi_{\mathrm{ox}}$ and $\Delta\psi_{\mathrm{NW}}$ are the surface potential changes at the solution–$SiO_2$ interface and at the NW, respectively. When $V_{lg}$ is swept from the subthreshold regime to the above-threshold regime, the increase in the electron carrier density of the n-type NW will result in an increase in $C_{NW}$, which will play an increasingly important role in determining the value of $\alpha$. As a result, the sensitivity of the NW device will decrease, due to the decrease in the coupling ratio, upon increasing the value of $V_{lg}$. Consequently, capacitive competition between $C_{NW}$ and $C_{ox}$ will govern the sensitivity of the NW biosensor in the high conductance regime, depending on the value of $V_{lg}$, in terms of the potential coupling ratio of $\Delta\psi_{\mathrm{NW}}$ to $\Delta\psi_{\mathrm{ox}}$.

Notably, a significant drop in sensitivity occurred in the low conductance regime, which can be regarded as the second stage (figure 5), presumably because the inherent conductance of the NW was comparable with the ionic conductance of the leakage paths through the solutions (about $4 \times 10^{-9}$ S in this study, as mentioned above). The measured conductance of the biosensor was contributed mainly by the parallel connection of the inherent conductance of the NW and the ionic conductance of the leakage paths. Therefore, the influence of the ionic conductance could not be neglected in the low conductance regime; as a result, the influence of the leakage paths will cause notable sensitivity degradation and will narrow the operating window in the subthreshold regime. Thus, the ionic conductance of the NW plays a significant role in determining the optimal sensitivity of NW biosensors operated in the subthreshold regime, especially in the case of biosensors incorporating NWs having low inherent conductance.

## 4. Conclusions

In summary, we have demonstrated that the sensitivity of an NW biosensor can be electrically modulated using liquid-gating. The surface potential change at the solution–$SiO_2$ interface, due to deprotonation, can also be extracted. The dependence of the sensitivity on the value of $V_{lg}$ originated from competition between $C_{NW}$ and $C_{ox}$, based on the equivalent capacitive model. The significant sensitivity degradation caused by the leakage paths through ionic solutions will narrow the operating window of biosensors operated in the low conductance regime. Our findings open

a window toward understanding how liquid-gating can be used to electrically modulate the sensitivities of biosensors to their limits, thereby allowing them to be applied to the promising field of ultrahigh-sensitivity biosensors.

## Acknowledgments

We thank Professor H C Lin and the National Nano Device Laboratories (NDL) for helpful assistance during device fabrication. This study was supported financially by the National Science Council (NSC99-2218-E-492-001 and NSC98-2321-B-009-001) and the Department of Health (DOH99-TD-N-111-003) of Taiwan.

## References

[1] Cui Y, Wei Q, Park H and Lieber C M 2001 *Science* **293** 1289
[2] Patolsky F, Zheng G, Hayden O, Lakadamyali M, Zhuang X and Lieber C M 2004 *Proc. Natl Acad. Sci.* **101** 14017
[3] Zheng G F, Patolsky F, Cui Y, Wang W U and Lieber C M 2005 *Nat. Biotechnol.* **23** 1294
[4] Patolsky F, Zheng G and Lieber C M 2006 *Nat. Protoc.* **1** 1711
[5] Stern E, Klemic J F, Routenberg D A, Wyrembak P N, Turner-Evans D B, Hamilton A D, LaVan D A, Fahmy T M and Reed M A 2007 *Nature* **445** 519
[6] Besteman K, Lee J, Wiertz F G M, Heering H A and Dekker C 2003 *Nano Lett.* **3** 727
[7] Yeh P H, Li Z and Wang Z L 2009 *Adv. Mater.* **21** 4975
[8] Hahm J I and Lieber C M 2004 *Nano Lett.* **4** 51
[9] Wang W U, Chen C, Lin K H, Fang Y and Lieber C M 2005 *Proc. Natl Acad. Sci.* **102** 3208
[10] Hsiao C Y, Lin C H, Hung C H, Su C J, Lo Y R, Lee C C, Lin H C, Ko F H, Huang T Y and Yang Y S 2009 *Biosens. Bioelectron.* **24** 1223
[11] Stern E, Steenblock E R, Reed M A and Fahmy T M 2008 *Nano Lett.* **8** 3310
[12] Chen Y, Wang X, Erramilli S, Mohanty P and Kalinowski A 2006 *Appl. Phys. Lett.* **89** 223512
[13] Gao X P A, Zheng G and Lieber C M 2010 *Nano Lett.* **10** 547
[14] Lu M P, Hsiao C Y, Lo P Y, Wei J H, Yang Y S and Chen M J 2006 *Appl. Phys. Lett.* **88** 053114
[15] Rosenblatt S, Yaish Y, Park J, Gore J, Sazonova V and McEuen P L 2002 *Nano Lett.* **2** 869
[16] Van Hal R E G, Eijkel J C T and Bergveld P 1996 *Adv. Colloid Interface Sci.* **69** 31
[17] Vu X T, Eschermann J F, Stockmann R, GhoshMoulick R, Offenhäusser A and Ingebrandt S 2009 *Phys. Status Solidi* a **206** 426
[18] Mai Anh T, Dzyadevych S V, Soldatkin A P, Duc Chien N, Jaffrezic-Renault N and Chovelon J M 2002 *Talanta* **56** 627